Improving spatiotemporal characterisation of cognitive processes with data-driven EEG-fMRI analysis.

Bogdan Mijović[1,2], Maarten De Vos[1,2,3], Katrien Vanderperren[1,2], Sabine Van Huffel[1,2]

[1]Katholieke Universiteit Leuven, Department of Electrical Engineering, ESAT-SCD, Leuven, Belgium

[2]IBBT-K.U.Leuven Future Health Department, Leuven, Belgium

[3]Oldenburg University, Department of Psychology, Neuropsychology Lab, Oldenburg, Germany

***Abstract* — To fully understand the cognitive processes occurring in the human brain, high resolution in both spatial and temporal information is needed. Most neuroimaging approaches, however, only possess high accuracy in one of these two domains. Therefore, the multimodal analysis of brain activity is becoming more and more popular among the research community. One of these approaches concerns the integration of simultaneously acquired electroencephalographic (EEG) and functional magnetic resonance imaging (fMRI) data. This combination poses a series of challenges, ranging from recovering data quality to the fusion of two types of data of a completely different nature. In this work, several of these challenges will be addressed, and an overview of different integration approaches is provided.**

I. INTRODUCTION

The synchronized relevant neural firing can be measured with the electroencephalogram (EEG) as event-related potentials (ERP) with high temporal resolution. This neural activity is also accompanied by a regional increase in cerebral blood flow, which can be indirectly measured as a Blood Oxygenation Level Dependant (BOLD) signal with functional Magnetic Resonance Imaging (fMRI). Contrary to EEG, fMRI has high spatial, but very low temporal resolution. Simultaneous measurement of the two can provide deeper insight into function and dysfunction of brain dynamics (Ullsperger, 2010) due to complementary nature of these signals.

In recent years, several integration approaches have been proposed. The earliest proposed methods were EEG-informed fMRI and fMRI-informed EEG analysis. These approaches are asymmetric, meaning that one of the modalities is considered to be prior knowledge to improve the results in the other modality.

Another set of integration approaches do not use one of the modalities as prior knowledge and are thus considered to operate more symmetrically. These approaches are therefore commonly referred to as EEG/fMRI fusion. Popular methods for this purpose are data-driven signal processing techniques, which are already well-established for processing EEG and fMRI separately. The advantage of simultaneous measurements has already been exploited in numerous cognitive neuroscience applications (the overview is provided in Ullsperger, 2010). There is also an increased trend of using integration techniques for medical application. For instance, the integration of EEG and fMRI allows localizing epileptic activity based on spike-triggered fMRI (Benar, 2006).

The goal of this work is to review necessary preprocessing techniques of the EEG and fMRI data, before the two can be integrated. Further, several integration and fusion techniques are explained and some results are shown to closer depict to the reader the possibilities of such integration.

II. EEG-FMRI DATA

Illustrations given in this paper come from EEG and fMRI data simultaneously acquired during a simple visual detection task. Quadrant segments of a circular checkerboard were projected from the technical room of the scanner to the plastic screen. They were presented equiprobable with randomized stimulus-onset asynchronies (SOAs) to each of four quadrants: upper left (UL), upper right (UR), lower left (LL), and lower right (LR). The subject was instructed to fixate the cross in the middle of the screen and to press a button whenever (s)he detected a checkerboard. The stimuli were presented in four blocks of 100 stimuli and 61 empty events each. The SOA varied randomly from 1 to 2.5 s in 100 ms steps. More details about the presentation paradigm can be found in (Novitskiy, 2011).

III. EEG PREPROCESSING

Gradient-artifact removal

When recorded simultaneously with fMRI, EEG data are highly contaminated with artifacts. Firstly, radio-frequency (RF) and gradient artifacts, which may have amplitudes 10 to 100 times larger than EEG signal itself, occur due to switching magnetic fields during fMRI acquisition. These artifacts occupy broad frequency spectrum, which overlaps with the frequency spectrum of the EEG information. Therefore, it is shown that fourth-order low-pass filtering with a cutoff point as low as 13 Hz cannot suppress imaging artifact in ECG signals and gives considerable ECG signal distortion (Felblinger, 1999). In this context, EEG and ECG signals have similar spectral content so similar results would be expected for EEG.

Nevertheless, since this artifact is invariant over time, subtracting procedure based on an average artifact template (proposed in Allen, (2000)) works reasonably well in most applications. This method consists of two stages. First, an average artifact waveform is calculated over a fixed number of epochs and in the second step, this waveform is subtracted from the EEG for each epoch. Adaptive noise canceling is then optionally used to attenuate any residual artifact. Fig. 1-a shows 5 seconds of the acquired EEG signal inside the magnetic field with gradients. The same EEG signal segment, after successful gradient artifact removal and low pass filtering (30*Hz*) is shown in Fig 1-b. One can observe that the amplitude of the signal is significantly reduced (from around 2mV down to only few micro-volts).

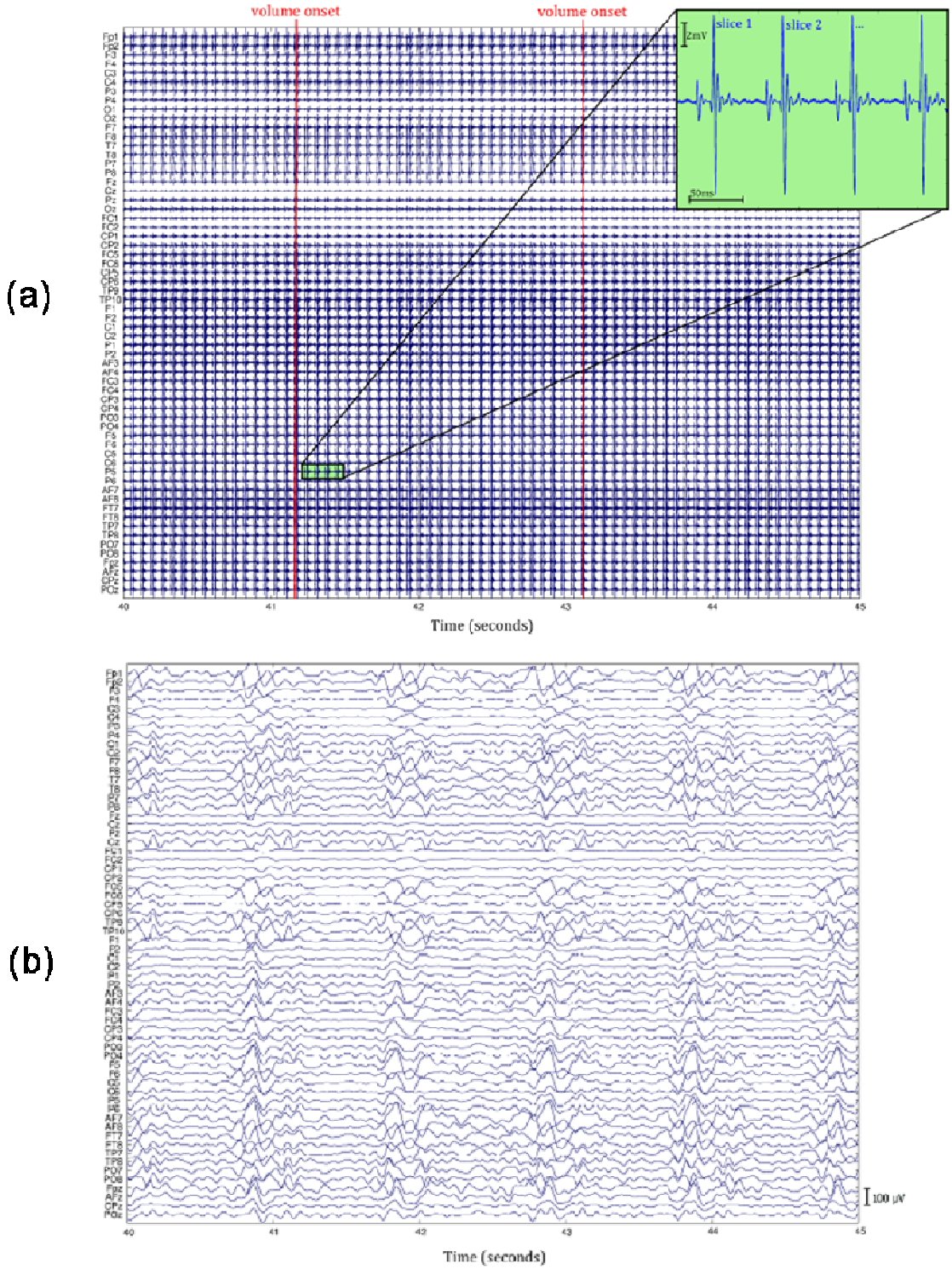


Fig. 1 (a) EEG data segment recorded inside the scanner with. Gradient artifacts are clearly visible. (b) EEG signal after gradient artifact reduction and low-pass filtering. The only residual artifact is the balistocardiogram artifact.

Ballistocardiogram artifact

A bigger challenge is posed by the ballistocardiogram (BCG) artifact, produced by cardiac pulse-related movement of the scalp electrodes inside the magnetic field. This artifact is still visible after gradient artifact has been removed (Fig. 1-b). With every heart beat, the electrodes are slightly displaced, therefore producing the artifact, which follows closely the QRS complex on the ECG lead. Therefore, measuring ECG inside the magnetic field and detection of the QRS complex helps with removing this artifact. Not only is the exact cause of this movement still a matter of investigation, the removal of this artifact is also a problematic issue, reported in many simultaneous EEG/fMRI studies (e.g. Debener, 2007). Many methods have already been proposed for this purpose. However, before the algorithms for BCG artifact reduction can be applied, the QRS events have to be properly detected.

For this reason, ECG is measured simultaneously with EEG with one lead, and the method for detecting QRS on this lead can be summarized as follows. The ECG data is first filtered, and then a complex ECG signal is constructed by applying the k-Teager energy operator. In this way a specific frequency is emphasized. Then, three different thresholds are computed from this complex signal, and QRS peaks are detected each time the amplitudes exceeds the sum of these three thresholds. Further details can be found in (Niazy, 2005).

Although this procedure showed high sensitivity and specificity in (Niazy, 2005), in our study the method failed in several datasets, meaning that the artifacts stayed partly misaligned. One of the shortcomings of this method is that only the ECG lead is used when generating the template for the alignment. Instead, since this artifact is also present on the EEG leads, the artifact template may be created taking more channels into account, therefore enhancing the correlation. The second problem might be the fact that an average template is used for the correlation and that this template is not updated in between the two alignment steps.

We, therefore, propose the improved iterative method for the correlation-based alignment (Vanderperren, 2011b), based on the following steps. If the initial detection is bad (i.e. more than 20% of the QRS are wrongly detected), the detection step can be performed taking either another electrode, or a set of additional electrodes. Afterwards, the detection should be checked for missing R-peaks, and these

should be added either automatically (e.g. based on a mean RR-distance), or manually. Redundant R-peaks also have to be removed. After all this has been done, the correlation-based alignment (including one or more EEG channels) can be performed again to correct the misaligned peaks.

The number of available segments (e.g. 100ms before until 500 ms after the presented stimulus) after thresholding at 50 μV is significantly better in the case with additional QRS correction compared to the case without (p-value of Wilcoxon signed rank test = 0.00001). Also at $100\mu V$ and $150\mu V$ there is a significant increase in number of segments (p = 0.0001 and p = 0.03 respectively). The regular QRS detection and the detection using our improved method are shown in Fig. 2.

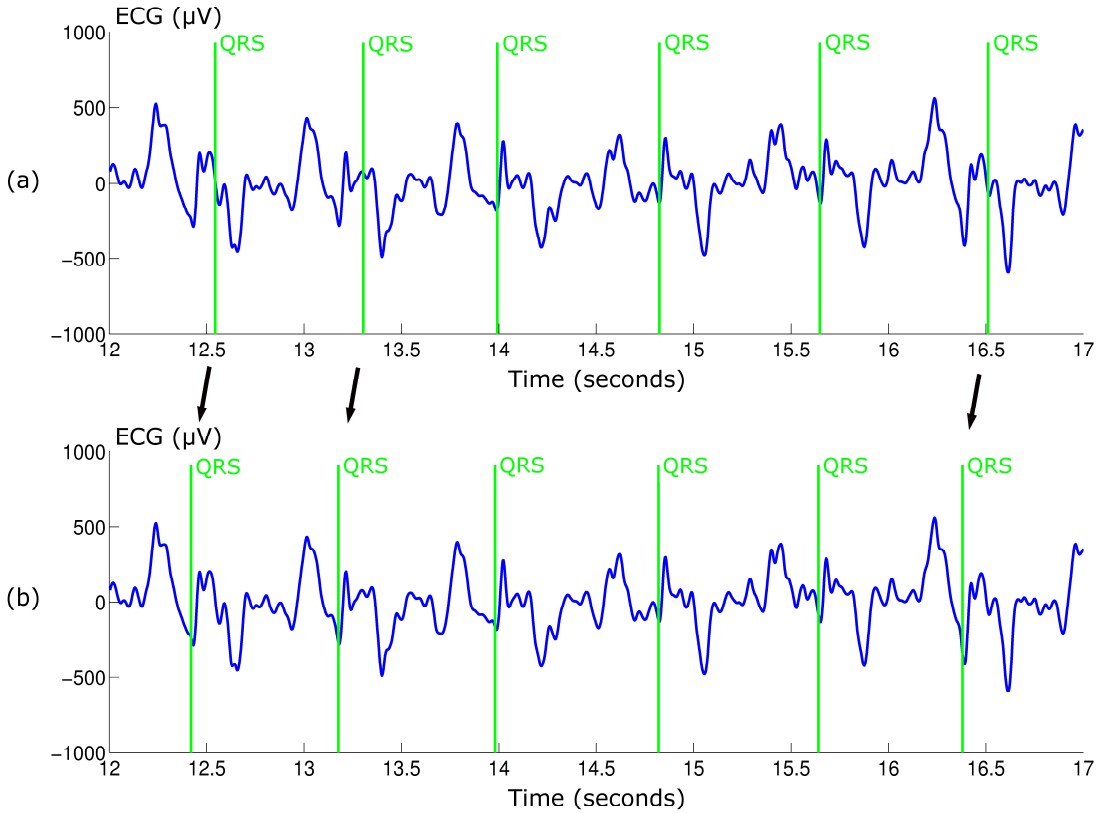


Fig. 2 (a) Five seconds fragment of ECG data with green marks corresponding to detected QRS complexes obtained with regular detection. Half of the detections in this data piece are differently aligned compared to the other half; (b) Same ECG fragment with new QRS timings obtained by following the step-by-step correction procedure.

Algorithms for the BCG-artifact removal

The algorithms for the BCG-artifact removal can be roughly subdivided in two groups. The first group of the algorithms is based on the channel-wise artifact template subtraction. The way this artifact template is generated differs among different approaches. The first study (Allen, 1998) aimed at constructing dynamic average artifact template (similar to what has been used for gradient artifact removal). Variations on this average template followed based on median-filtering (Elingson, 2004) and Gaussian weighted averaging (Goldman, 2000). Finally, Optimal Basis Set (OBS) of principal components for the template creation is suggested (Niazy, 2005). This technique relies on the idea that principal component analysis (PCA) applied to all artifact occurrences in each channel separately makes it possible to capture the temporal variations of the BCG artifact. The resulting averaged ERP over one subject with its standard deviation is shown in Fig. 3 before and after BCG removal. It is apparent that the standard deviation significantly reduces. This is especially obvious during the prestimulus interval (-100ms – 0 ms), where the baseline is flat after the BCG artifact is removed, whereas the oscillations are visible when the OBS is not performed.

The methods from the second group are based on blind source separation (BSS) techniques. Several algorithms can be used for this purpose. The most widely reported blind source separation technique for BCG artifact removal is Independent Component Analysis (ICA) (Srivastava, 2005; Benar, 2006; Mantini, 2007). This method is used to recover underlying sources of the recorded data, assuming that these sources are mutually statistically independent. ICA applied to EEG data contaminated with BCG artifacts can potentially identify both brain- and artifact related sources, given that they are independent, thereby cleaning up the EEG by removing the artifactual sources.

However, most ICA algorithms assume stationarity of the underlying sources. Since the BCG artifact shows a considerable spatial variation across its occurrence (Vanderperren, 2010), satisfying this assumption can be problematic. For this reason, it was suggested to apply OBS prior to ICA (Debener, 2005), instead of applying ICA directly on the EEG data. This approach would combine the strengths of both methods, removing the major part of the artifact with OBS and its residuals with ICA.

In (Vanderperren, 2010), several methodological issues are clarified regarding the different approaches with an extensive validation based on ERPs. Also the advantages of applying ICA after OBS is discussed and compared. Most attention in this work was focused on task-related measures, including their use on trial-to-trial information. Both OBS and ICA proved to be able to yield equally good results. However, ICA methods needed more parameter tuning, thereby making OBS more robust and easy to use.

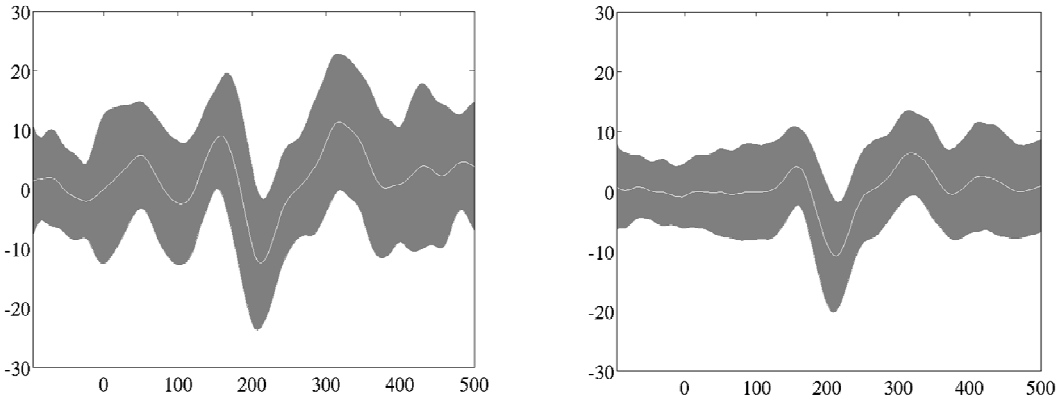


Fig. 3 Averaged single-subject ERP (white) with its standard deviation (gray) over trials before removing the BCG artifact with the OBS method (left). The average ERP of the same subject after the BCG artifact removal is shown in the right panel.

IV. FMRI DATA

Preprocessing:

When it comes to preprocessing the fMRI data, other difficulties are encountered. Several steps are required from acquisition of the fMRI image, until the data can be fused with ERPs. These steps we review shortly in the following steps.

The acquisition of one complete fMRI volume requires the successive acquisition of a specific number of slices, and the whole volume is acquired in around 2 to 3 seconds. This means that the difference in time when the first slice and the last slice are acquired is at the order of 2 seconds. Therefore, in some studies, the “slice time correction” is applied to compensate for this delay.

After the slice time correction, the “spatial realignment” of the acquired images has to be performed. Although all the necessary measures have been taken to prevent the head motion, displacements up to

several millimeters can still occur. This can lead to unwanted changes in some voxels, and therefore this has to be corrected for. What is most commonly used in practice is to select one acquired volume as a reference scan, and to realign all the other volumes to this reference volume.

The corregistration with the anatomical image can also be applied. This step can even be skipped, but it is useful to visualize the brain activations overlaid over the anatomical image. A rigid-body transformation is used for co-registration, including three translations and three rotations along the different axes.

To compare the results obtained in different subjects, it is necessary to map all of their brains into the same space. Usually, all the brains are mapped into a common template space (e.g. Montreal Neurological Institute (MNI) template). This process of mapping all the brains into the same template is called normalization. The normalization can be applied to either anatomical or functional images.

After all these steps, the functional images are usually spatially smoothed. The smoothing is achieved by convolving the fMRI image by a Gaussian kernel of a specified width. This step is mostly performed to artificially introduce more correlations between the neighboring voxels, which is important in the following step, where the active voxels are identified through statistical analysis.

Statistical Analysis

The aim of the statistical analysis of the fMRI data is to locate the voxels with statistically significant change in oxygen over time, corresponding to the time-course of the presented stimuli. Most commonly, a mass-univariate approach based on general linear model is used for this purpose.

First, a regressor is made as a stick function, having ones at the time-instants when the stimuli were presented and zeros otherwise. Then, this stick function is convolved with the model of the model of a hemodynamic response function (HRF) to create the model of the BOLD response. This model is then fit into the GLM, and the T-values are computed. The active voxels are defined as the ones that are significantly different from zero (usually $p<0.05$).

V. EEG-FMRI FUSION

The idea of making a relationship between (integrating) measured EEG and fMRI signals is supported by the research of Logothetis (2001), who showed in macaque monkeys that the local field potential (LFP) recordings correlate linearly with the BOLD signal. Since then, for integration of the simultaneously recorded EEG and fMRI signals in humans, several approaches have been proposed. Most commonly, presented approaches can be divided in three different groups.

The first group represents the integration-by-prediction approaches (or EEG-informed fMRI analysis). In this type of analysis, certain features of the single trial ERP components are used as predictors (regressors) for the statistical fMRI analysis. This approach is schematically presented in Fig. 4 (figure borrowed from Debener, 2006). One can use the changes in only one of the ERP components. In Debener (2005) for instance, the amplitude of the N1 component – the minimum of the interval of 15-85 ms is determined, and then the mean of the preceding (-80ms-0) and succeeding (85-200ms) positivity windows are subtracted. The computed values are subsequently used as regressors for fMRI analysis. Other studies combined two ERP component features. In (Karch, 2010) it was shown that N2- and P3- based fMRI analysis shows activations in different brain areas, corresponding to different aspects of voluntary selection. In (Novitskiy, 2011), the P1- and N1- based regressors were used to separate the activations of the visual system at the latency of 100-200 ms. Also the combination of three regressors can also be used, like in (Eichele, 2005), where P2- (170ms), N2- (200 ms), and P3- (320ms) based regressors predicted spatially different patterns during auditory oddball task . The features used for regressors in this kind of analysis are usually amplitudes, as mentioned above, but latencies of the certain components can also be used (e.g. Benar, 2007; Warbrick, 2009). The main challenge of the integration by prediction approaches is to try to find the feature, upon it is possible to disentangle the trial-by trial fluctuations of different peaks. This problem is also addressed in (Vanderperren, 2011a).

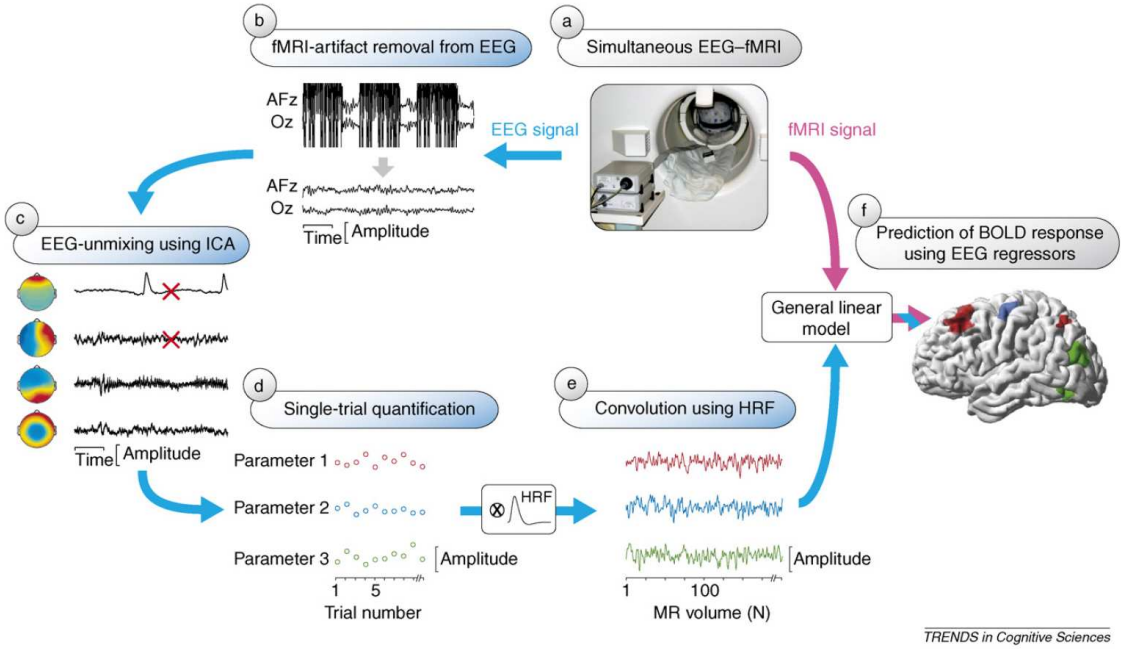


Figure 4. The EEG-informed fMRI analysis. EEG and fMRI data are recorded simultaneously. After acquisition, the EEG data follows the blue-arrow preprocessing path. The fMRI data is added only after the EEG data features are extracted and convolved with the hemodynamic response function. The fMRI data follows the pink arrow path.

The second group of EEG-fMRI integration approaches consists in fMRI-informed EEG analysis approaches. In these approaches, the information obtained from the fMRI measurements is used to constrain the equivalent dipole or distributed estimates of the EEG sources. In (Bledowski, 2004) the P300 generators are localized in visual target and distractor processing. Another application is shown in (De Martino, 2011), where relevance vector machines are used to predict single-trial ERP responses from the fMRI measurements.

The obvious drawback of these two groups of approaches is, however, that they force the information from one modality onto another one. Therefore, these approaches cannot be considered full integration approaches, since there is no temporal forward model that will start from both information, and fuse them in the sense that it exploits the underlying dynamics of both of them symmetrically.

The third group of integration approaches consists in the joint data-driven analysis of ERP and fMRI maps derived from the response to a particular stimulus. Several methods have already been proposed for this purpose, and they can be based on modeling (as in e.g. Daunizeau, 2007), or blind source separation

(BSS) techniques, such as independent component analysis (ICA) or canonical correlation analysis (CCA). These methods employ both modalities at the same time, and therefore are usually referred to EEG/fMRI fusion methods.

An example of model-based approaches is given by Daunizeau, (2007). In that work, Variational Bayesian learning scheme is exploited to retrieve the common EEG-fMRI information from the joint EEG-fMRI dataset. The model follows the assumption that the temporal and spatial information can be separated. A common spatial profile is extracted, since this profile is introduced as unknown hierarchical prior on both (EEG and fMRI) markers of cerebral activity. The method is first assessed through simulation data, and thereafter verified in the EEG and fMRI recordings of an epileptic patient, where the intracranial EEG recordings are used for validation.

The CCA-based approach to fusion is presented in (Correa, 2008, 2010). Given the two datasets X_1 and X_2, CCA tries to find linear combinations X_1W_1 and X_2W_2 that maximize the pair-wise correlation. In this approach, X_1 and X_2 are the set of average ERPs and task-related fMRI contrast maps over subjects. In (Correa, 2008) for example, it is shown using this method, that the N2 and P3 ERP peaks during the auditory oddball task are related with temporal and motor areas in fMRI. A more general correlation-based method is proposed in (Martinez-Montes, 2004). In that work 3-dimensional EEG (subjects x time x frequency) and fMRI (subjects x time x space) data are used (see also De Vos, 2007). It is shown that alpha-band activity of EEG is closely correlated with the temporal activity of fMRI, thereby activating parieto-occipital complex, thalamus and insula.

Besides the above-mentioned CCA approaches, different ICA approaches have also been proposed. Contrary to the CCA, ICA employs measures of higher order statistics independence, rather than just second-order statistics (correlation). The ICA approaches can be divided in two groups – Parallel and Joint ICA approaches. In parallel ICA approaches the data for both modalities are first preprocessed separately, and then the connections between the modalities are made afterwards. In (Eichele, 2008), after the independent components are extracted, the relations are made based on correlations between trial-to-trial fluctuations in the time domain (Fig. 6). The drawback of this method, however, is that it does not allow any interference between modalities during the decomposition step.

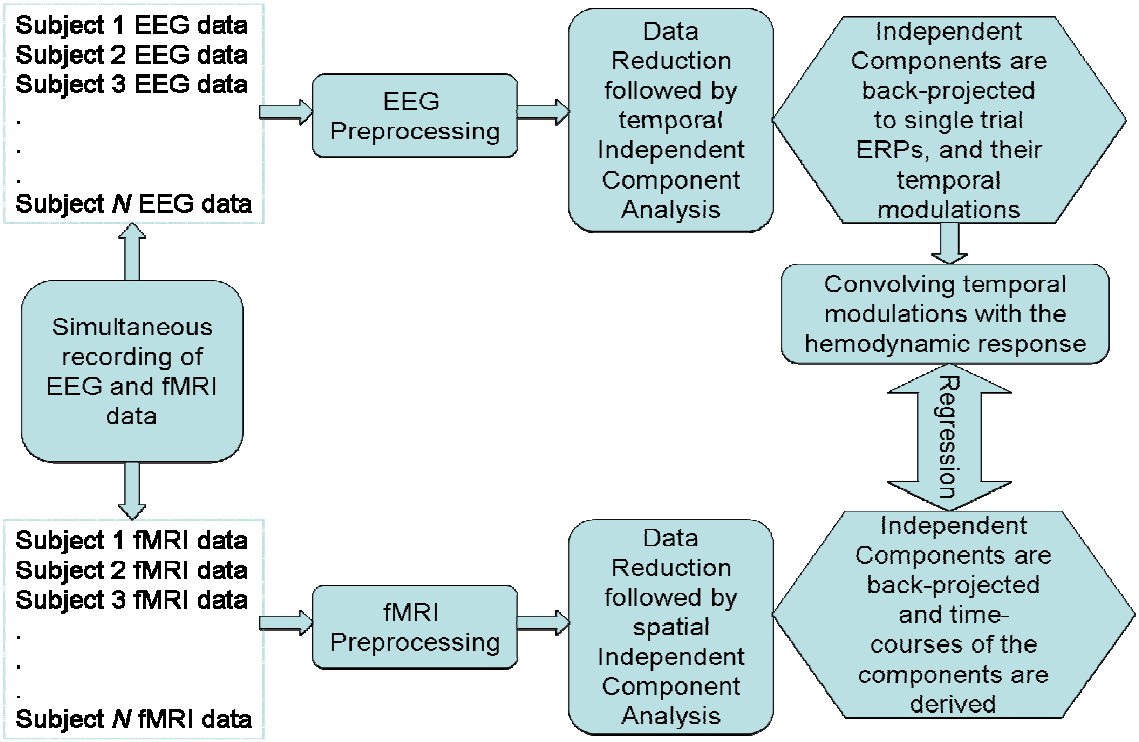


Figure 6. Schematic representation of the ParallelICA algorithm, proposed by Eichele, (2008). It is apparent from the picture that the EEG and fMRI data are first preprocessed separately, and the connections are defined only in the last step – regression.

Another parallel ICA approach has been proposed in (Lei, 2010). This approach is very similar to the previous one, with a difference that the components are linked in spatial and temporal model using variational Bayesian techniques. This allows results for one modality to be used as priors for another one (results from ICA decomposition of the EEG modality can be used as priors for fMRI and vice versa). This fact makes this method integration, rather than data-fusion approach. In (Lei, 2010) the simulation study is provided and the results are discussed.

The parallel approach which imposes constraints during the parallel decomposition is proposed in (Liu, 2007). As in previous cases, this approach also applies the ICA algorithm to the two modalities separately. However, contrary to other ParallelICA approaches, the correlations between the corresponding mixing vectors of the two modalities are forced during the separate decompositions.

Therefore, the connections are made more symmetrically than in the above-mentioned parallel ICA approaches.

Another interesting fusion approach to this problem is called joint independent component analysis (JointICA) (Calhoun, 2006; Mijovic, 2011). JointICA identifies the independent components of both modalities simultaneously, and connects them in an integrated fMRI-ERP result, where each fMRI independent component is associated to an ERP-derived time course. This approach is schematically shown in Fig. 6. The method assumes that the different wave components (peaks) of the ERP and the spatial components in a statistical brain activation map (activation sites) of the same stimulus co-vary. This is either because they are generated in the same brain region or because the BOLD active areas had participatory roles in ERP activity, without necessary being the source of a particular ERP wave.

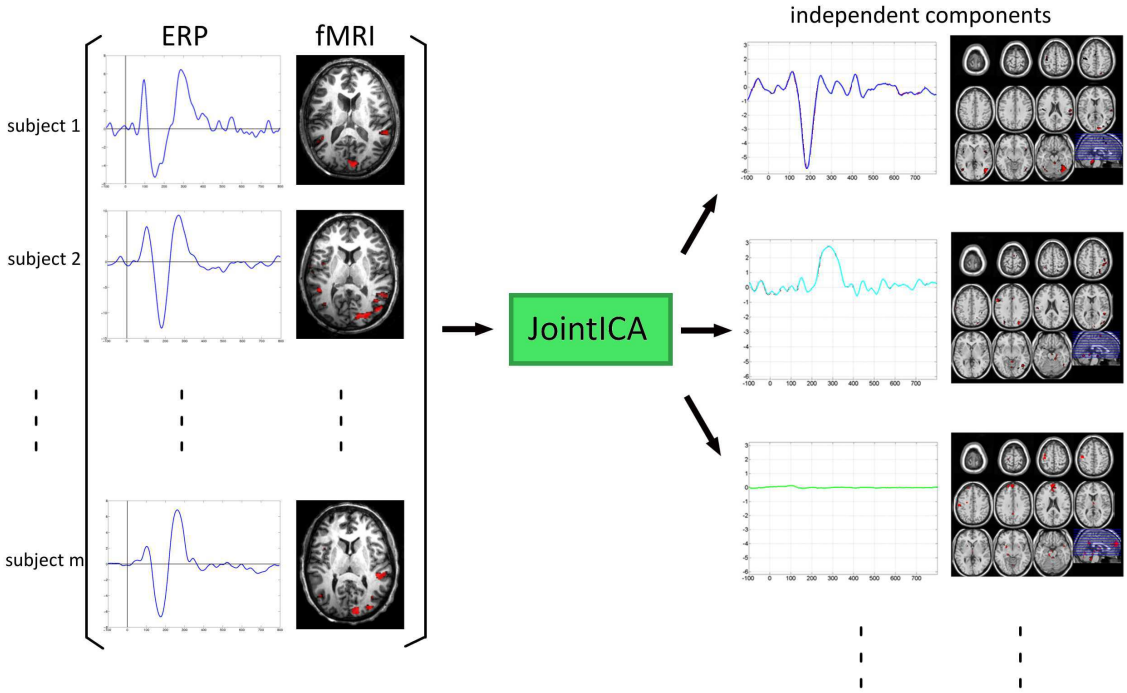


Fig. 6 Schematic representation of the application of the JointICA method to average ERPs and fMRI maps from m subjects. On the left the matrix with the concatenated ERP and fMRI data per subject is shown, which is (after upsampling of the ERPs and normalization) fed into JointICA. On the right some examples of resulting components are presented, each consisting of an ERP and an fMRI part.

Fig. 7 shows the performance of the JointICA algorithm performed on data obtained from the described visual detection task. The same visual paradigm was used in (Di Russo, 2003) and the ERP generators are estimated using the dipole modeling procedure. The first occipital component (corresponding to the C1 ERP wave) is expected in the primary visual cortex, around the calcarine sulcus. In that study, the P1 ERP wave is expected to be generated by two areas. One of the components is expected to originate from the fusiform gyrus, generating the early P1 component, and another one in the medial occipital gyrus, generating late P1 component. The P2 component is generated in precuneus and cuneus.

Fig. 7 shows that the same findings can be obtained by JointICA. In this way, the path of the visual signal can be shown. Moreover, Fig. 7 shows that the N1 component also covariates with the motor activity (as mentioned before, in this task the subject is requested to press a button), although the ERP data are recorded on the occipital PO8 and Oz electrodes. Therefore, JointICA can be viewed as an exploratory tool for exploring brain activity using multimodal measurements, thereby exploiting both high spatial resolution of fMRI and temporal resolution of the EEG measurements.

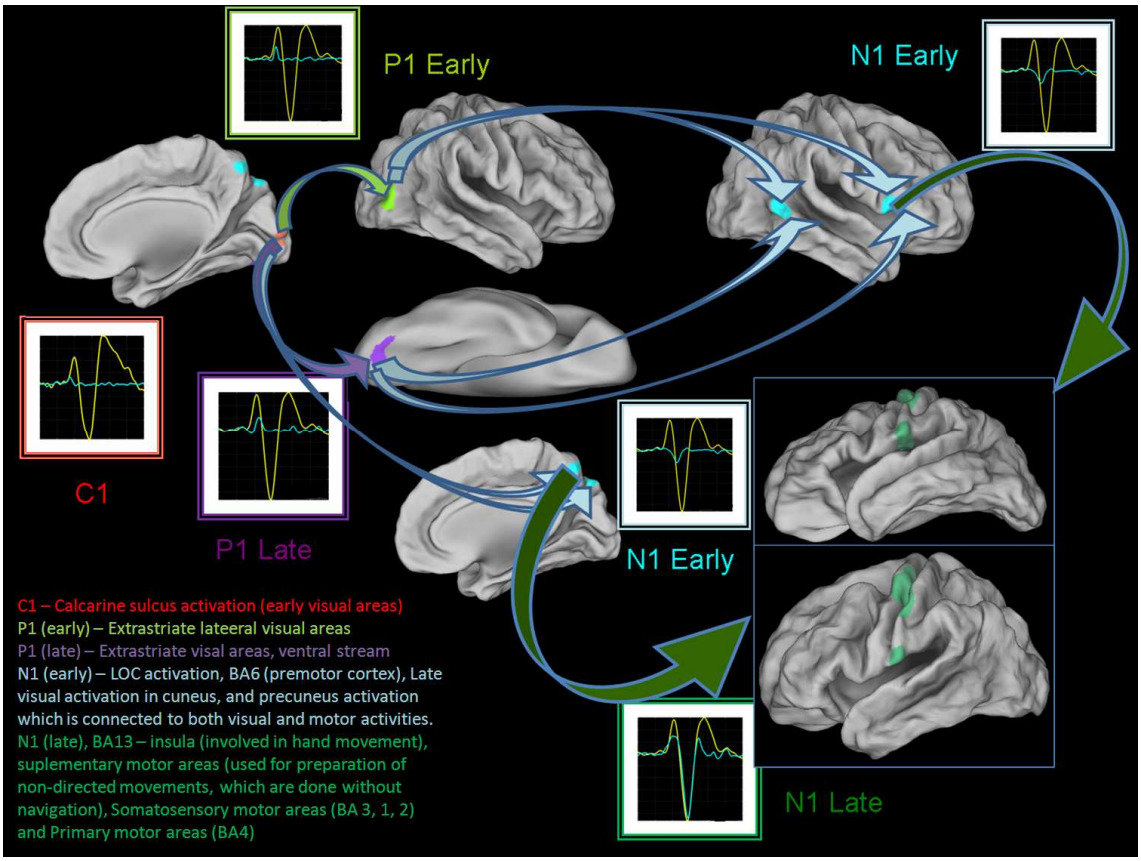


Fig 7. Visual path, derived from visual detection task, where the subject was instructed to press a button each time a stimulus appears. The activations are separated using JointICA technique.

VI. CONCLUSION

In conclusion, the simultaneous EEG-fMRI recordings combine two very important markers of brain activity. These recordings also allow for enhancing the spatio-temproal resolution, with which the brain activity can be observed. Several integration techniques have already been proposed for this purpose. Some of these techniques are overviewed in this article, together with the necessary preprocessing schemes for each modality. The underlying assumptions for several integration and fusion techniques are explained and discussed. Also the results obtained from these algorithms are described, and the possibilities for applications are illustrated.

VII. ACKNOWLEDGEMENTS

This research is supported by the Research Council KUL: GOA-AMBio-RICS, GOA MaNet and CoE EF/05/006; the Belgian Federal Science Policy Office IUAP P6/04 (DYSCO, Dynamical systems, control and optimization, 20072011); the Flemish Government: G.0427.10N Integrated EEG-fMRI, IWT-TBM080658-MRI and IBBT; and the EU project Neuromath (COSTBM0601).

Katrien Vanderperren is supported by a PhD grant from the Agency for Innovation by Science and Technology (IWT).

Maarten De Vos is supported by an Alexander von Humboldt grant.

The scientific responsibility is assumed by its authors.

REFERENCES

1. Allen, P.J., Josephs, O., Turner, R., *A Method for Removing Imaging Artifact from Continuous EEG Recorded during Functional MRI*. NeuroImage 12, 2000, 230-239
2. Allen, P.J., Polizzi, G., Krakow, K., et al., *Identification of EEG events in the MR scanner: the problem of pulse artifact and a method for its subtraction*. NeuroImage 8, 1998, 229–239
3. Bénar C G, Grova C, Kobayashi E, et al., *EEG–fMRI of epileptic spikes: Concordance with EEG source localization and intracranial EEG.* NeruoImage 30 (4),1996, 1161-1170.
4. Benar, C. G., Schon, D., Grimault, S., Nazarian, B., Burle, B., Roth, M., et al., *Single-trial analysis of oddball event-related potentials in simultaneous EEGfMRI*. Human Brain Mapping 28, 2007, 602-613.
5. Bledowski, C., Prvulovic, D., Hoechstetter, et al., *Localizing P300 generators in visual target and distractor processing: a combined event-related potential and functional magnetic resonance imaging study*. J Neurosci 24, 2004, 9353-9360.
6. Calhoun V D, Adali T, Pearlson G D, and Kiehl K A (2006). Neuronal chronometry of target detection: Fusion of hemodynamic and event-related potential data. NeuroImage 30, 544-553.
7. Calhoun, V.D., Adali, T., Pearlson, G.D., Kiehl K.A., *Neuronal chronometry of target detection: Fusion of hemodynamic and event-related potential data*. NeuroImage 30, 2006, 544-553.

8. Correa, N., Li, Y.O., Adali, T., Calhoun, V.D., *Canonical Correlation Analysis for Data Fusion and Group Inference*. IEEE Signal Proc. Mag. 39, 2010, 39-5
9. Correa, N.M., Li, Y.O., Adali, T., Calhoun, V.D., *Canonical Correlation Analysis for Feature-Based Fusion of Biomedical Imaging Modalities and Its Application to Detection of Associative Networks in Schizophrenia*. IEEE J. Sel. Top. Signa. 2 (6), 2008, 998-1007
10. Daunizeau, J., Grova, C., Marrelec, G., Mattout, J., Jbabdi, S., Pélégrini-Issac, M., et al., *Symmetrical event-related EEG/fMRI information fusion in a variational Bayesian framework,* NeuroImage, 36(1), 2007, 69-87.
11. De Martino, F., de Borst, A.W., Valente, G., et al., *Predicting EEG single trial responses with simultaneous fMRI and relevance vector machine regression.* NeuroImage 56 (2), 2011, 826-836.
12. De Vos M., Vergult A., De Lathauwer L., De Clercq W., Van Huffel S., Dupont P., Palmini A., Van Paesschen W., *Canonical decomposition of ictal scalp EEG reliably detects the seizure onset zone*, NeuroImage, 37 (3) , 2007, 844-854
13. Debener, S., Strobel, A., Sorger, B, et al., *Improved quality of auditory event-related potentials recorded simultaneously with 3 T fMRI: removal of the ballistocardiogram artifact.* NeuroImage 34, 2007, 587–597.
14. Debener, S., Ullsperger, M., Siegel, M., Fiehler, K., von Cramon, D.Y., Engel, A.K. *Trial-by-trial coupling of concurrent electroencephalogram and functional magnetic resonance imaging identifies the dynamics of performance monitoring.* J. Neurosci. 25 (50), 2005, 11730–11737.
15. Debener, S., Ullsperger, M., Siegel, M., Engel, A.K., *Single-trial EEG–fMRI reveals the dynamics of cognitive function*. Trends in Cognitive Sciences 10 (12), 2006, 558-563.
16. Di Russo, F., Martinez, A., Hillyard, S.A., *Source analysis of event-related cortical activity during visuo-spatial attention.* Cereb. Cortex 13, 2003, 486-499.
17. Eichele, T., Calhoun, V.D., Moosmann, M., Specht, K., Jongsmae, M.L.A., Quian Quiroga, R., et al., *Unmixing concurrent EEG-fMRI with parallel independentcomponent analysis.* Int. J. Psychophysiol. 67 (3), 2008, 222–234.

18. Eichele, T., Specht, K., Moosmann, M., et al., *Assessing the spatiotemporal evolution of neuronal activation with single-trial event-related potentials and functional MRI*. Proc Natl Acad Sci U S A 102, 2005, 17798-17803.

19. Ellingson, M.L., Liebenthal, E., Spanaki, M.V., Prieto, T., Binder, J.R., Ropella, K.M., *Ballistocardiogram artifact reduction in the simultaneous acquisition of auditory ERPS and fMRI*. NeuroImage 22, 2004, 1534–1542.

20. Felblinger, J., Slotboom, J., Kreis, R., et al., *Restoration of electrophysiological signals distorted by inductive effects of magnetic field gradients during MR sequences*. Magn.Reson. Med. 41, 1999, 715–721.

21. Goldman, R.I., Stern, J.M., Engel, J.Jr., Cohen, M.S., *Acquiring simultaneous EEG and functional MRI*. J. Clin. Neurophysiol. 111, 2000, 1974–1980.

22. Karch, S., Feuerecker, R., Leicht, G., Meindl, T., Hantschk, I., Kirsch, V., et al., *Separating distinct aspects of the voluntary selection between response alternatives: N2- and P3-related BOLD responses*. Neuroimage 51(1), 2010, 356-364.

23. Lei, X., Qiu, C., Xu, P., Yao, D., *A parallel framework for simultaneous EEG/fMRI analysis: methodology and simulation*. NeuroImage 52 (3), 2010, 1123-1134

24. Liu, J., Calhoun, V., 2007. *Parallel independent component analysis for multimodal analysis: Application to fMRI and EEG Data. Biomedical Imaging*. From Nano to Macro, 4th IEEE International Symposium on , 2007, 1028-1031

25. Logothetis, N.K., Pauls, J., Augath, M., et al., *Neurophysiological investigation of the basis of the fMRI signal*. Nature 412, 2001, 150-157.

26. Mantini, D., Perrucci, M.G., Cugini, S., Ferretti, A., Romani, G.L., Del Gratta, C., *Complete artifact removal for EEG recorded during continuous fMRI using independent component analysis.* NeuroImage 34, 2007, 598–607.

27. Martinez-Montes, E, Valdés-Sosa, P.A., Miwakeichi, F., et al., *Concurrent EEG/fMRI analysis by multiway Partial Least Squares.* NeuroImage 22 (3), 2004, 1023-1034.

28. Mijovic, B., Vanderperren, K., Novitskiy, N., Vanrumste, B., Stiers, P., Van den Bergh, B., et al. *The "Why" and "How" of JointICA: Results from a Visual Detection Task*. NeuroImage, 2011, (in revision).

29. Niazy, R.K., Beckmann, C.F., Iannetti, G.D., et al., *Removal ofFMRI environment artifacts from EEG data using optimal basis sets*. NeuroImage 28, 2005, 720–737

30. Novitskiy, N., Ramautar, J.R., Vanderperren, K., De Vos, M., Mennes, M., Mijovic, B., et al., *The BOLD correlates of the visual P1 and N1 in single-trial analysis of simultaneous EEG-fMRI recordings during a spatial detection task*. NeuroImage, 54(2), 2011, 824-835

31. Srivastava, G., Crottaz-Herbette, S., Lau, K.M., et al., *ICA-based procedures for removing ballistocardiogram artifacts from EEG data acquired in the MRI scanner*. NeuroImage 24, 2005, 50–60

32. Ullsperger, M., Debener, S., Simultaneous EEG and fMRI, Recording, Analysis and Application. Oxford University Press (New York), 2010.

33. Vanderperren, K., Ramautar, J., Novitski, N., De Vos, M., Mennes, M., Vanrumste, B., et al., 2007. *Ballistocardiogram artifacts in simultaneous EEG-fMRI acquisitions*. Int. J. Bioelectromagn. 9 (3), 146–150 Special Issue on Methods for the estimation of brain activity I.

34. Vanderperren K, De Vos M, Ramautar J R, Novitskiy N, Mennes M, Assecondi S, et al., *Removal of BCG artifacts from EEG recordings inside the MR scanner: a comparison of methodological and validation-related aspects*. NeuroImage 50(3), 2010, 920-934.

35. Vanderperren, K., Mijovic, B., Novitskiy, N., Vanrumste, B., Stiers, P., Vand den Bergh, B., et al., *Single trial ERP reading based on Parallel Factor Analysis.* Psychophysiology, submitted, 2011a.

36. Vandereprren K., *Improving data-driven EEG-fMRI analyses for the study of cognitive functioning*, PhD Thesis, Katholieke Universiteit Leuven, Belgium, 2011b.

37. Warbrick, T., Mobascher, A., Brinkmeyer, J., Musso, F., Richter, N., Stoecker, T., et al., *Single-trial P3 amplitude and latency informed event-related fMRI models yield different BOLD response patterns to a target detection task.* Neuroimage 47, 2009, 1532-1544

Author: Bogdan Mijović

Email: bogdan.mijovic@esat.kuleuven.be

Institution Address: Kasteelpark Arenberg 10, 3001 Heverlee

Country:Belgium